# Transitional nuclei in the rare-earth region: Energy levels and structure of $^{130,132}$Ce, $^{132,134}$Nd, and $^{134}$Pm, via $\beta$ decay of $^{130,132}$Pr, $^{132,134}$Pm, and $^{134}$Sm

M. O. Kortelahti*
*Louisiana State University, Baton Rouge, Louisiana 70803*

B. D. Kern
*University of Kentucky, Lexington, Kentucky 40506*

R. A. Braga and R. W. Fink
*School of Chemistry, Georgia Institute of Technology, Atlanta, Georgia 30332*

I. C. Girit†
*UNISOR and Vanderbilt University, Nashville, Tennessee 37235*

R. L. Mlekodaj†
*UNISOR, Oak Ridge Associated Universities, Oak Ridge, Tennessee 37831*

(Received 18 April 1990)

An investigation of low-lying energy levels of $^{130,132}$Ce, $^{132,134}$Nd, and $^{134}$Pm has been made via $\beta$ decay, especially of those levels in the $K^\pi=2^+$ gamma band in the even-even nuclei. The radioactive parent nuclei were produced by the $^{92}$Mo($^{46}$Ti,*xpyn*) and $^{112}$Sn($^{28}$Si,*xpyn*) reactions with bombarding energies of 170 to 240 MeV. An isotope separator enabled $A=134$ mass identification. Level schemes of these five nuclei were constructed from $\gamma$-$\gamma$-$t$ coincidence data. The $\beta$-decay half-lives of the parent nuclei, $^{130}$Pr, $^{132}$Pr, $^{132}$Pm, $^{134}$Pm, and $^{134}$Sm, were determined to be 40±4, 96±18, 8.8±0.8, 23±2, and 9.3±0.8 s, respectively. The suitability of the proton-neutron interaction boson model in describing $^{130}$Ce, $^{132}$Ce, $^{132}$Nd, and $^{134}$Nd is supported by the comparison of experimental relative $E2$ transition probabilities with proton-neutron interaction boson model predictions.

MS code no. CR4132 1990 PACS number(s): 23.20.Ck, 23.20.Lv, 27.60.+j, 23.40.Hc

## I. INTRODUCTION

In the region where neutron-deficient nuclei have $Z>50$ and $N<82$, there are many nuclei whose systematic progression from vibrational to gamma-soft rotor to possible rigid rotator types is of interest.[1–5] The neutron-deficient even-$Z$, even-$N$ Ce, Nd, and Sm nuclei do not show the striking effects that are seen in the neutron-rich region of Nd and Sm nuclei due to the subshell closure at $Z=64$. Rather, a smooth increase in deformation occurs as the neutron number decreases. Previous in-beam spectroscopy studies of Ce even-even isotopes,[6,7] Nd isotopes,[8] and Ce to Gd isotopes[9] have shown, through the transitions from high-spin states, that the even-even nuclei in this region become more deformed as the neutron number decreases from approximately $N=80$ to 68. The energies of the $2^+$ and $4^+$ levels of the ground-state band decrease monotonically through the known region. Early work on the levels and structure of $^{130,132}$Ce, $^{132,134}$Nd, and $^{134}$Pm is reviewed elsewhere.[10–12] Recent relevant reports on the beta decay of $^{132,134}$Pm and levels of $^{132,134}$Nd are given in Refs. 13–15. Relevant energy levels of $^{130}$Ce are described in Ref. 16. We earlier made a brief report[17] on the levels of the four even-$Z$, even-$N$ nuclei of this paper.

In this paper are described data to assist in evaluating the structure of nuclei in this region; they have been acquired through the heavy-ion beam production of radioactive $^{130,132}$Pr, $^{132,134}$Pm, and $^{134}$Sm and the observation of their subsequent beta decay. Typically, many more low-lying low-spin levels are populated via $\beta$ decay than in the in-beam experiments. A previous paper in this series[18] showed that the relative $B(E2)$'s of decays of the gamma-band levels in $^{136}$Nd indicate agreement with a gamma-soft nuclear model. The current paper includes proton-neutron interaction boson model (IBM-2) calculations of $B(E2)$ transition probabilities in $^{126,128,130,132,134,136}$Ce, $^{132,134,136,138}$Nd, and $^{134,136,138,140}$Sm. Comparisons are made between calculated $B(E2)$ ratios and experimental ratios for $\gamma$-ray transitions from gamma-band energy levels. This work extends that of Casten and von Brentano[19] who reported on Xe and Ba nuclei near $A=130$.

A level scheme for $^{134}$Pm is presented.

## II. EXPERIMENTAL METHODS

The apparatus and techniques that were used in our previous studies of Nd, Pm, and Sm nuclei in this region have been described elsewhere (Refs. 18, 20–23, and references therein), and all details will not be repeated here. The folded-tandem accelerator of the Holifield Heavy-Ion Research Facility at Oak Ridge National Laboratory provided beams for these reactions: (a) $^{112}$Sn

 

($^{28}$Si,$xnyp$) at beam energies of 170, 190, and 220 MeV with targets enriched to 80% in $^{112}$Sn; (b) $^{92}$Mo($^{46}$Ti,$xnyp$) at 250 MeV with targets enriched to 97.4% in $^{92}$Mo; and (c) $^{92}$Mo($^{46}$Ti,$xnyp$) at 230 MeV with UNISOR mass separation. Radioactive products were transported by a He-jet system to a continuous thin plastic foil on which they were repeatedly collected and then transported to a $\gamma$-ray counting station. Two Ge detectors were used, as described in Ref. 18, to obtain $\gamma$-$\gamma$-$t$ and $X$-$\gamma$-$t$ coincidence spectra as well as singles spectra. The collection and counting times were equal and varied from 7 to 175 s. Mass separation with the UNISOR magnetic isotope separator[20,21] was carried out in obtaining additional $A=134$ coincidence and singles spectra, with reaction (c).

## III. EXPERIMENTAL RESULTS

### A. $^{134}$Pm $\xrightarrow{\beta}$ $^{134}$Nd and levels of $^{134}$Nd

The prominent $\gamma$ rays of $^{134}$Nd were observed at $A=134$ (Fig. 1) during the mass separator experiment. The He-jet measurements produced a substantial increase in $\gamma$-ray yield from which $\gamma$-$\gamma$ coincidence spectra were extracted from the event-by-event mode data. The 294.4-keV $\gamma$ ray was used to gate the spectrum shown in Fig. 2, and then each of the $\gamma$ rays in that spectrum were used as gates. The spectra gated by all other significant $\gamma$ rays were checked for relevancy. These spectra were acquired in 7 h of counting time with the 20-s collect/count cycle, with reaction (a) at a beam energy of 190 MeV. The energies, relative intensities of the $\gamma$-ray transitions, and the $\gamma$-$\gamma$ coincidences are listed in Table I.

The level diagram of Fig. 3 was constructed using the relative intensities and the singles and $\gamma$-$\gamma$ coincidence relationships. Tentative spin-parity assignments in $^{134}$Nd can be made with reference to the systematic trends in neighboring nuclei. The existence of a ground-state band with $0^+$, $2^+$, $4^+$, and $6^+$ levels is well known, having been observed both in $\beta$ decay and in the in-beam yrast cascades. Assignment of the 754.0-keV level as the $2^+_\gamma$ band head for the gamma band is reasonable for a nucleus in this region. This assignment is supported by the presence of other probable members of a gamma band with spin parities from $3^+$ to $6^+$. The choice of levels for the gamma band, up to $6^+$, are shown in Fig. 3. There is good agreement with an earlier level scheme[13] in which the $2^+$ and $3^+$ levels of the gamma band were tentatively identified, and also with the recent one of Vierinen *et al.*[14] The gamma-band assignments are consistent with the $2^+$, $4^+$, and $6^+$ spin parities recently given[24] to levels at 753, 1312, and 1908 keV. The $5^-$ and $7^-$ levels were earlier reported[15] as the lower levels of an yrast band going up to $13^-$.

The half-life of the $\beta$ decay of $^{134}$Pm was measured by observing the decay with time of the yields of the 294.4- and 495.1-keV $\gamma$ rays, which are shown in Fig. 4. The average value is 23±2 s, in good agreement with 21±1 s reported by Béraud *et al.*[13] and with 22.6±0.5 s reported by Vierinen *et al.*[14] The populating of the $4^+$ and $6^+$ levels of the ground-state band of $^{134}$Nd indicates that $\beta$ decay of $^{134}$Pm occurs from a relatively high-spin state with probable $I^\pi=5^+$ (for allowed $\beta$ decay) with the observed 23-s half-life. The relatively weak observed $\beta$ de-

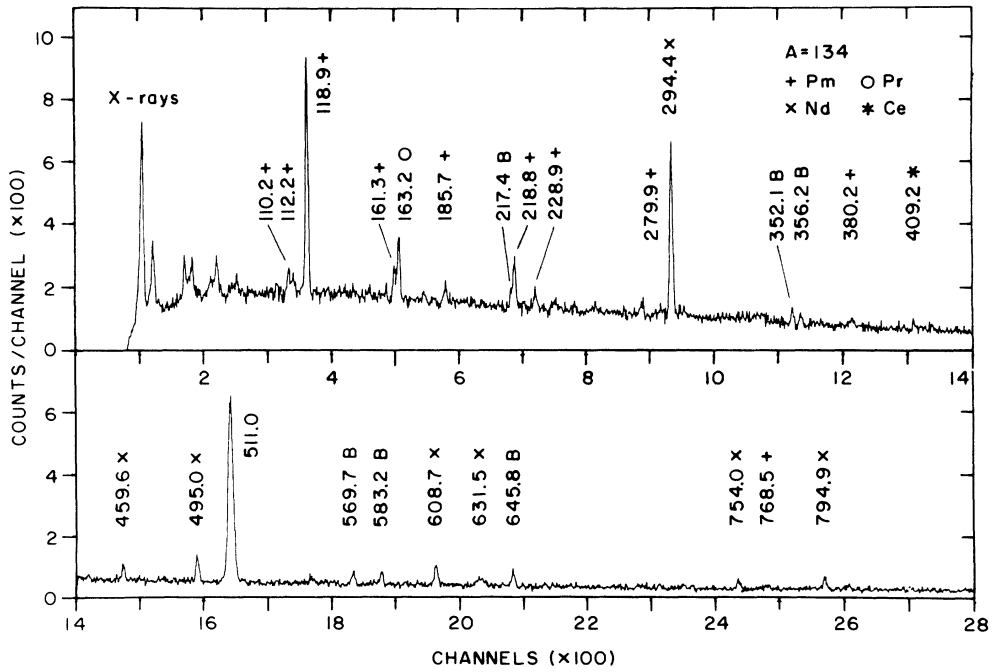


FIG. 1. Spectrum of $\gamma$ rays from the $\beta$ decay of mass-separated $A=134$ nuclei, acquired with use of the UNISOR mass separator during the first 3 s of counting in each cycle. The prominent 118.9- and 294.4-keV $\gamma$ rays are due to the $\beta$ decay of $^{134}$Sm and $^{134}$Pm, respectively. "*B*" indicates background lines.

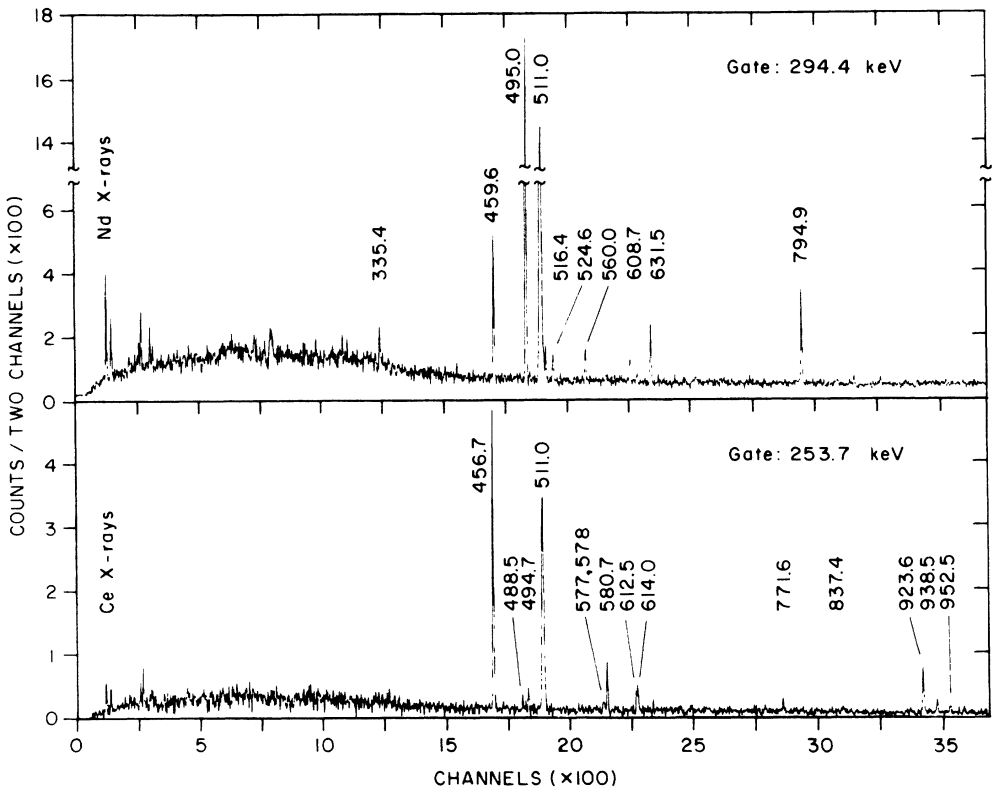


FIG. 2. (a) Spectrum gated by the 294.4-keV $\gamma$ ray due to the $\beta$ decay of $^{134}$Pm to $^{134}$Nd. (b) A spectrum gated by the 253.7-keV $\gamma$ ray due to the $\beta$ decay of $^{130}$Pr to $^{130}$Ce. Spectra (a) and (b) were acquired with reaction (a) at beam energies of 190 and 220 MeV, respectively, with use of the He-jet facility.

TABLE I. Energies, relative intensities, and $\gamma$-$\gamma$ coincidences of the $\gamma$ rays, which were observed following the $\beta$ decay of $^{134}$Pm to $^{134}$Nd. The relative intensities were extracted from data that were produced by the $^{112}$Sn($^{28}$Si,*xnyp*) reaction at bombarding energy of 190 MeV. The relative intensities may be different for other reactions due to probable differences in the population of the $^{134}$Pm isomers. Uncertainty in the last digit is given in the parentheses.

| $E_\gamma$ (keV) | Relative intensity ($I_\gamma$) | Coincident x and gamma rays |
|---|---|---|
| 294.4 (2) | 100 (5) | Nd x rays, 335.4, 459.6, 495.0, 516.4, 524.6, 560.0, 597.0, 608.7, 631.5, 794.9, 851.8, 881.9, 1166.8, 1247.3 |
| 335.4 (2) | 4.8 (7) | 294.4, 459.6, 516.4, 608.7, 754.0 |
| 459.6 (2) | 14.2 (7) | 294.4, 335.4, 516.4, 560.0, 608.7, 851.8 |
| 495.0 (2) | 56.7 (3) | 294.4, 524.6, 631.5, 881.9, 1166.8, 1247.3 |
| 516.4 (2) | 2.1 (3) | |
| 524.6 (2) | 2.9 (3) | 294.4, 495.0 |
| 560.0 (2) | 9.4 (8) | 294.4, 459.6, 597.0, 754.0 |
| 597.0 (2) | 1.3 (5) | |
| 608.7 (2) | 3.8 (4) | 294.4, 335.4, 754.0, 794.9 |
| 631.5 (2) | 9.7 (6) | 294.4, 495.0 |
| 754.0 (2) | 14.2 (7) | 335.4, 516.4, 560.0, 608.7, 851.8 |
| 794.9 (2) | 18.4 (9) | 294.4, 516.4, 608.7 |
| 851.8 (2) | 5.2 (10) | 294.4, 459.6, 754.0 |
| 881.9 (4) | 1.8 (5) | 294.4, 495.0 |
| 1166.8 (2) | 5.3 (7) | 294.4, 495.0 |
| 1247.3 (2) | 2.9 (10) | |

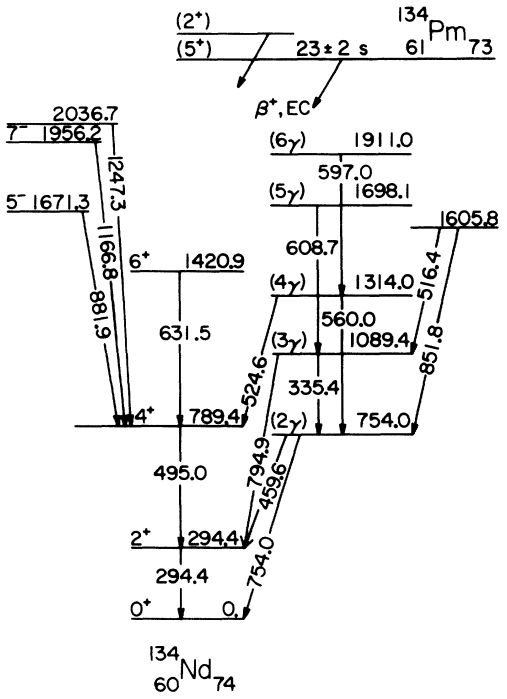


FIG. 3. Partial energy level diagram of $^{134}$Nd due to the $\beta$ decay of $^{134}$Pm. The $I^{\pi}$ assignments are discussed in the text. The energies are in keV. The parentheses indicate that an experimental determination of $I^{\pi}$ has not been made.

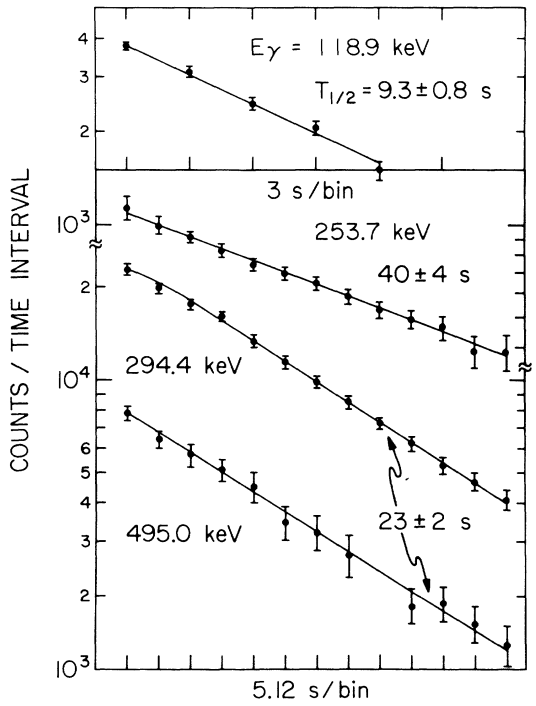


FIG. 4. Decay of selected $\gamma$ rays due to the $\beta$ decay of $^{134}$Sm (118.9 keV), $^{134}$Pm (294.4 and 495.0 keV), and $^{130}$Pr (253.7 keV). The $\gamma$ ray yields were extracted from time-tagged spectra.

cay directly to the $2_g^+$ level indicates decay from a low-spin isomer of $^{134}$Pm, which is discussed in Sec. III B. The half-life of this low-spin isomer was not detectable.

### B. $^{134}$Sm $\xrightarrow{\beta}$ $^{134}$Pm and levels of $^{134}$Pm

Spectra collected with the mass separator at $A=134$ contained x-ray lines of Pm, singly and in coincidence with the previously known 118.9 keV $\gamma$ ray, and thus the previous identifications of the $\beta$ decay of $^{134}$Sm were confirmed. An example is shown in Fig. 1. Coincidence spectra were gated by the x rays, the 118.9-keV $\gamma$ ray, and other $\gamma$ rays. Additional coincidence spectra collected by use of the He-jet technique at beam energies of 190, 220, and especially 250 MeV supported the assignments and relative intensities, and enabled somewhat better determinations of the energies. The $\gamma$-$\gamma$ coincidences related to $^{134}$Pm are given in Table II. Through use of the $\gamma$-ray singles intensities and the $\gamma$-$\gamma$ coincidence relationships, the partial energy level diagram of Fig. 5 was constructed. The 112.2-KeV $\gamma$ ray decays with the same half-life as the 110.2-keV $\gamma$ ray. Since it is in coincidence with the 218.8-keV $\gamma$ ray but not with the 118.9-keV $\gamma$ ray, it has been placed tentatively as a transition to the ground state. The $\gamma$ rays in Fig. 5, and some others which we did not observe, were reported recently by Vierinen *et al.*[14]

The half-life for the $\beta$ decay of $^{134}$Sm, measured by the intensity of the 118.9- and 161.3-keV $\gamma$ rays, is 9.3±0.8 s, in agreement with the previous 12±3 s (Ref. 25) and 10.3±0.5 s.[14] The decay curve for the 118.9-keV $\gamma$ ray is included in Fig. 4.

An approximate log$ft$ of 5.2 was calculated with use of the systematic value of the maximum positron energy, 6 MeV,[26] and the deduced 23% $\beta$ feeding to the 118.9-keV

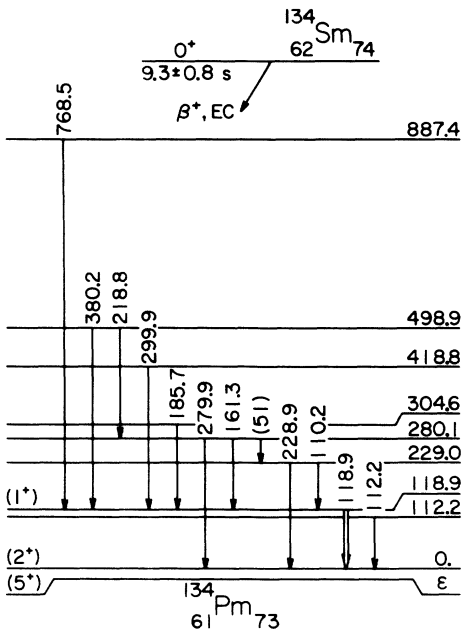


FIG. 5. Partial energy level diagram of $^{134}$Pm due to the $\beta$ decay of $^{134}$Sm. The magnitude and sign of $\epsilon$ are not known.

TABLE II. Energies, relative intensities, and $\gamma$-$\gamma$ coincidences of the $\gamma$ rays which were observed following the $\beta$ decay of $^{134}$Sm to $^{134}$Pm. Uncertainty in the last digit is given in the parentheses.

| $E_\gamma$ (keV) | Relative intensity ($I_\gamma$) | Coincident x and $\gamma$ rays |
|---|---|---|
| 51 (2) | | |
| 110.2 (2) | 9 (2) | Pm x rays, 118.9, 218.8 |
| 112.2 (2) | 6 (1) | Pm x rays |
| 118.9 (2) | 100 (5) | Pm x rays, 51, 110.2, 161.3, 185.7, 218.8, 299.9, 380.2, 768.5 |
| 161.3 (5) | 20 (5) | Pm x rays, 118.9, 218.8 |
| 185.7 (3) | 13 (1) | 118.9 |
| 218.8 (2) | 33 (3) | Pm x rays, 51, 110.2, 112.2, 118.9, 161.3, 228.9, 279.9 |
| 228.9 (3) | 14 (1) | 51, 218.8 |
| 279.9 (3) | 14 (1) | 218.8 |
| 299.9 (3) | 12 (2) | 118.9 |
| 380.2 (2) | 17 (2) | 118.9 |
| 768.5 (3) | 6 (2) | 118.9 |

level. Allowed $\beta$ decay to the 118.9-keV level is indicated, and this suggests that this level has spin parity $1^+$, because $0^+ \xrightarrow{\beta} 0^+$ $\beta$ decay is rare (allowed $\beta$ decay is assumed). A reasonable choice for the lowest level of Fig. 5 is $I^\pi=2^+$, which requires an $M3/E4$ transition to or from the $5^+$ isomeric level, as was discussed in Sec. III A. It is not known which level is the lower in energy, the presumed $2^+$, which is connected to other levels of the decay scheme, or the presumed $5^+$, which appears to be produced directly by the $^{92}$Mo ($^{46}$Ti, $3pn$) reaction.

The similarity of the distribution of low-lying levels and their energies to those of $^{136}$Pm suggests[18] that the same quasi-single-particle proton and neutron states are coupling to produce the same (as yet unidentified) multiplets.

### C. $^{132}$Pm $\xrightarrow{\beta}$ $^{132}$Nd and levels of $^{132}$Nd

From Ref. 9 it was known that the energies of the $\gamma$ rays from the $2^+$, $4^+$, and $6^+$ levels of the ground-state band of $^{132}$Nd have energies of 213.1, 397.0, and 522.0-keV. The $\gamma$-ray energies, relative intensities, and coincidence relationships listed in Table III were derived from coincidence spectra and from singles spectra, especially with reaction (a) at 190 MeV and 20-s cycle time. They were confirmed with use of reaction (b) at 250 MeV and 7-s cycle time. The coincidence relationships and relative intensities of the $\gamma$ rays were used in constructing the level diagram of Fig. 6. The 522.0-keV $\gamma$ ray was not seen. The 294.1-keV transition was indicated by the coincidence data; its intensity is uncertain because of interference caused by the strong 294.4-keV $\gamma$ ray of $^{134}$Nd.

The observed levels strongly suggest that the $\beta$-decay parent has a low spin with $I=3$ as a most probable choice. The half-life of the $\beta$ decay of $^{132}$Pm was determined from the yield of the 213.1-keV $\gamma$ ray versus time as $8.8\pm0.8$ s, using reaction (b) at 250 MeV and 35-s cycle time with confirmation from using reaction (a) at 170 and 190 MeV. The only previous measurement is that of Wilmarth *et al.*,[27] who gave $5.0\pm0.7$ s.

### D. $^{132}$Pr $\xrightarrow{\beta}$ $^{132}$Ce and levels of $^{132}$Ce

The members of the ground-state band of $^{132}$Ce are known from in-beam measurements[6,7] and the second $2^+$ level from $\beta$ decay.[25] Subsequent to our brief description[17] of the $\beta$ decay, Barnéoud *et al.*[28] added transitions to our $^{132}$Ce level diagram. Our best yield was obtained with reaction (b) at 250 MeV, with a cycle time of 175 s,

TABLE III. Energies, relative intensities, and $\gamma$-$\gamma$ coincidences of the $\gamma$ rays which were observed following the $\beta$ decay of $^{132}$Pm to $^{132}$Nd. Uncertainty in the last digit is given in the parentheses.

| $E_\gamma$ (keV) | Relative intensity ($I_\gamma$) | Coincident x and $\gamma$ rays |
|---|---|---|
| 213.1 (2) | 100 (10) | Nd x rays, 294.1, 397.0, 564.5, 610.4, 904.5 |
| 294.1 (4) | 1 (0.5) | 213.1 |
| 397.0 (2) | 26 (3) | 213.1 |
| 564.5 (3) | 3 (1) | 213.1, 610.4, 823.5 |
| 610.4 (3) | 14 (2) | 213.1, 294.1, 564.5 |
| 823.5 (3) | 13 (2) | |
| 904.5 (2) | 7 (1) | 213.1 |

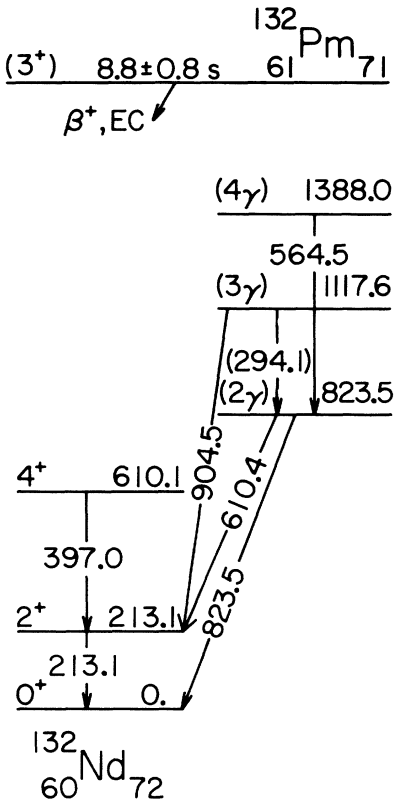


FIG. 6. Partial energy level diagram of $^{132}$Nd due to the $\beta$ decay of $^{132}$Pm.

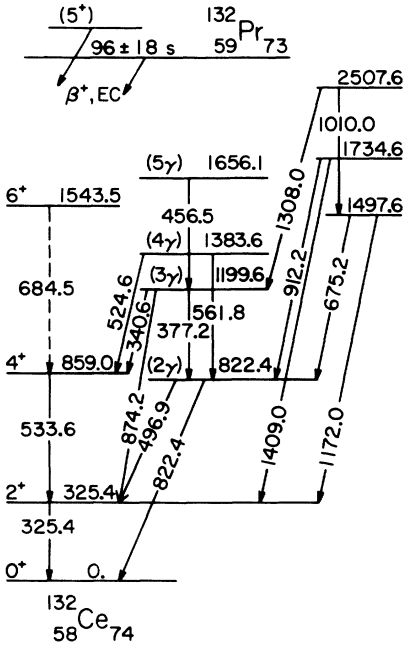


FIG. 7. Partial energy level diagram of $^{132}$Ce due to the $\beta$ decay of $^{132}$Pr.

which enhanced the 96-s half-life yield relative to other shorter-lived nuclei. The relative intensities were measured under these conditions. Table IV gives the $\gamma$-ray energies, relative intensities, and coincidence relationships.

The decay scheme of Fig. 7 has additions and changes that were made possible by new data, which were obtained using reaction (a) at 250 MeV. The level diagram is drawn to exhibit the gamma band consisting of the $2_\gamma$ to $5_\gamma$ levels. This diagram is consistent with the one recently reported.[28] In our work, the known 684.5-keV $\gamma$ ray from the $6^+$ level was observed as a very weak doubtful transition. Because of observed $\beta$ decay to spin-5 and possibly spin-6 levels, and also directly to the $2_g^+$ level, it appears that there are $\beta$-decay isomers; a reasonable tentative choice for the high-spin isomer is $I^\pi = 5^+$ and for the low-spin isomer, $I^\pi \leq 2^+$.

The yield versus time of the 325.4-keV $\gamma$ ray was seen to consist of a growth and decay which is consistent with $^{132}$Pr being fed by the 105-s $\beta$ decay of $^{132}$Nd while decaying with the 96-s half-life earlier reported.[25]

### E. $^{130}$Pr $\xrightarrow{\beta}$ $^{130}$Ce and levels of $^{130}$Ce

The most useful spectra were obtained with reaction (a) with beam energies of 190 and 220 MeV and cycle time of 20 s; see, for example, in Fig. 2 the spectrum gated by the 253.7-keV $\gamma$ ray. Spectra gated by the 253.7-keV $\gamma$ ray with use of reaction (a) at 190 and 220 MeV, and with reaction (b), exhibit the same coincidences for the more prolific $\gamma$ rays. At 220-MeV bombarding energy the spectrum showed only a very small amount of the contaminating $^{136}$Sm $\gamma$ ray of 256.0 keV. Energies and relative intensities are listed in Table V, where the intensities

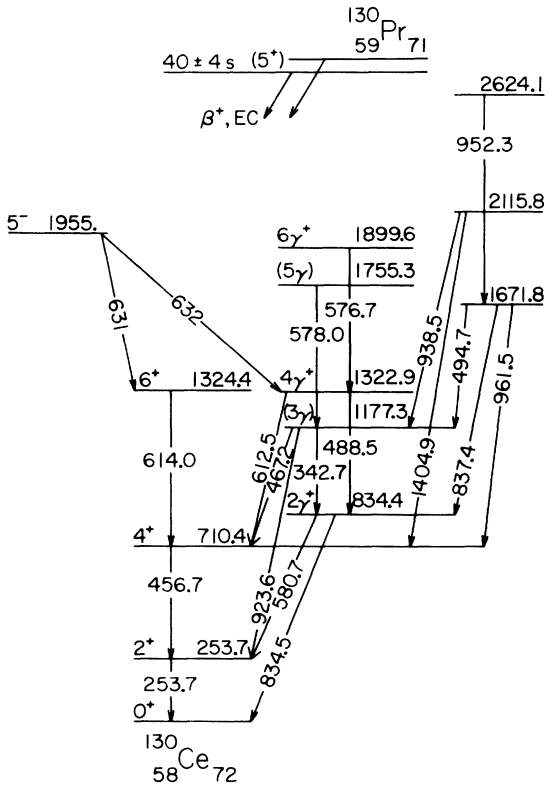


FIG. 8. Partial energy level diagram of $^{130}$Ce due to the $\beta$ decay of $^{130}$Pr.

TABLE IV. Energies, relative intensities, and $\gamma$-$\gamma$ coincidences of the $\gamma$ rays which were observed following the $\beta$ decay of $^{132}$Pr to $^{132}$Ce. Uncertainty in the last digit is given in the parentheses.

| $E_\gamma$ (keV) | Relative intensity ($I_\gamma$) | Coincident x and $\gamma$ rays |
|---|---|---|
| 325.4 (2) | 100 (5) | Ce x rays, 340.6, 496.9, 533.6, 561.8, 675.2, 684.5, 874.2, 912.2, 1010.0, 1172.0, 1308.0, 1409.0 |
| 340.6 (5) | <0.5 | |
| 377.2 (2) | 3.5 (8) | 325.4 |
| 456.5 (4) | 3.0 (8) | 325.4, 377.2, 822.4, 874.2 |
| 496.9 (2) | 25 (3) | 325.4, 377.2, 561.8, 675.2, 912.2, 1010.0 |
| 524.6 (2) | 2.0 (6) | 325.4, 533.6 |
| 533.6 (2) | 15.2 (15) | 340.6, 325.4, 524.6 |
| 561.8 (2) | 2.7 (6) | 325.4, 496.9, 822.4 |
| 675.2 (2) | 6.3 (8) | 325.4, 496.9, 822.4 |
| 684.5 | <0.5 | |
| 822.4 (2) | 17.3 (17) | 377.2, 561.8, 675.2, 912.2, 1010.0 |
| 874.2 (2) | 14.1 (14) | 325.4, 456.5 |
| 912.2 (2) | 3.4 (10) | 325.4, 496.9, 822.4 |
| 1010.0 (9) | 2.6 (5) | |
| 1172.0 (6) | 1.0 (5) | |
| 1308.0 (6) | 1.5 (3) | 325.4, 496.9, 874.2 |
| 1409.0 (8) | 1.5 (5) | |

are those observed with reaction (b) at 190 MeV. The low-lying spin-2 levels as well as the $6^+$ levels are fed by $\beta$ decay, indicating that a low-spin and a high-spin isomer are decaying.

The level scheme of Fig. 8 was constructed with use of the $\gamma$-ray energies, coincidences, and relative intensities which are listed in Table V. It has been arranged to emphasize the details associated with the gamma band. The spin parities of the $2^+_\gamma$, $4^+_\gamma$, and $6^+_\gamma$ of the gamma band were taken from Ref. 29 where they are the lower members of a band extending up to $14^+$. Additional data have made possible some additions and changes in our

TABLE V. Energies, relative intensities, and $\gamma$-$\gamma$ coincidences of the $\gamma$ rays which were observed following the $\beta$ decay of $^{130}$Pr to $^{130}$Ce. Uncertainty in the last digit is given in the parentheses.

| $E_\gamma$ (keV) | Relative intensity ($I_\gamma$) | Coincident x and $\gamma$ rays |
|---|---|---|
| 253.7 (2) | 100 (5) | Ce x rays, 342.7, 456.7, 467.2, 488.5, 494.7, 576.7, 580.7, 612.5, 614.0, 631.5, 837.4, 923.6, 938.5, 952.3, 961.5, 1404.9 |
| 342.7 (6) | 1.0 (3) | |
| 456.7 (2) | 38 (3) | 253.7, 467.2, 612.5, 614.0, 961.5 |
| 467.2 (6) | 1.3 (4) | |
| 488.5 (2) | 1.8 (3) | 253.7, 576.7, 580.7, 632.0, 834.5 |
| 494.7 (2) | 2.0 (6) | 253.7, 923.6, 952.3 |
| 576.7 (6) | 1.3 (4) | |
| 578.0 (3) | 0.4 (1) | |
| 580.7 (2) | 10.4 (10) | 253.7, 342.7, 488.5, 494.7, 837.4, 952.3 |
| 612.5 (3) | 2.6 (6) | 253.7, 456.7 |
| 614.0 (2) | 6.5 (6) | 253.7, 456.7, 631 |
| 631.5 (5)[a] | 1.3 (4) | 253.7, 456.7, 614.0 |
| 834.5 (2) | 8.0 (9) | 488.5, 837.4, 952.3 |
| 837.4 (2) | 7.7 (4) | 253.7, 580.7, 834.5 |
| 923.6 (2) | 13.8 (10) | 253.7, 494.7, 578.0, 938.5, 952.3 |
| 938.5 (2) | 3.4 (7) | 253.7, 923.6 |
| 952.3 (3) | 5.3 (7) | 253.7, 580.7, 834.5 |
| 961.5 (4) | 1.7 (6) | 253.7, 456.7 |
| 1404.9 (10) | 2.9 (9) | |

[a]Weak doublet.

previously published level scheme.[17] The expected $2\gamma^+ \rightarrow 0_g^+$ transition giving an 834.5-keV $\gamma$ ray was observed in the coincidence spectra gated by the 837.4-keV precursor, which itself appears in the spectrum gated by the 253.7-keV $\gamma$ ray. The $3_\gamma^+ \rightarrow 2_\gamma^+$ transition (342.7 keV), generally seen in the gamma band, is only weakly seen in spectra because of the competition given by the 923.6-keV $\gamma$ ray from the same level. The very weak 578.0- and 576.7-keV $\gamma$ rays are interpreted as coming from the $5_\gamma^+$ level at 1755.3 keV and the $6_\gamma^+$ level at 1899.6 keV, respectively. The level diagram is consistent with the pertinent part of the diagram, which was reported by Nolan *et al.*;[16] the definite $I^\pi$ values (i.e., those not in parentheses) are taken from that work. Our decay scheme is consistent with the recently published scheme due to Barnéoud *et al.*[28]

The $\beta$-decay half-life was determined from the decay of the 253.7-keV $\gamma$ ray to be 40±4 s. The decay is illustrated in Fig. 4.

## IV. CALCULATIONS

### A. IBM-2 calculations

IBM-2 calculations were made for the primary objective of extracting $E2$ transition rates to use in forming transition rate ratios which may be compared with the new experimental data of this paper and with other existing data. It is of interest to see if the strong systematic behavior which was reported[19] for the Xe and Ba nuclei with $N_n < 82$ is continued for Ce, Nd, and Sm.

$B(E2)$'s for the $N_n < 82$ Xe, Ba, and Ce nuclei were calculated by Puddu, Scholten, and Otsuka,[30] in an IBM-2 model. They adopted a smoothly varying set of IBM parameters (dependent on neutron number) and did not attempt to fit each nucleus individually. Our IBM-2 calculations have used their parameters as a starting point. The program NPBOS was used.[31] Not all of the terms in the NPBOS Hamiltonian were used. The Hamiltonian was limited to

$$H=\epsilon_d(n_{d\nu}+n_{d\pi})+\kappa(\mathbf{Q}_\nu\cdot\mathbf{Q}_\pi)+\mathbf{M}_{\nu\pi}+\mathbf{V}_{\nu\nu}+\mathbf{V}_{\pi\pi}\ , \quad (1)$$

in which there are 13 adjustable parameters: $\epsilon_d$, $\kappa$, and $\chi_\nu$ in $Q_\nu$ and $\chi_\pi$ in $Q_\pi$; $\xi_{1,2,3}$ in the Majorana term $M_{\nu\pi}$; $c_\nu^{(0,2,4)}$ in the $V_{\nu\nu}$ term; and $c_\pi^{(0,2,4)}$ in the $V_{\pi\pi}$ term. The operators are given in Ref. 31 and conveniently described in a review article by Arima and Iachello.[32] Input data were the known experimental values for the energies of the $2_g^+$, $4_g^+$, and $6_g^+$ levels and sometimes the $8_g^+$ level of the ground-state band, and the energies of available $2_\gamma^+, 3_\gamma^+, 4_\gamma^+, \ldots$ levels of the gamma band. Input data also included the experimental values of the ratio

$$R=\frac{B(E2;2_\gamma^+\rightarrow 0_g^+)}{B(E2;2_\gamma^+\rightarrow 2_g^+)}\ . \quad (2)$$

Another restriction was the requirement that the experimental $B(E2;0_g\rightarrow 2_g)$ be reproduced by the calculations; because they depend on the choice of effective charge, it was a less rigorous constraint. The number of proton bosons was given by $N_\pi=(N_p-50)/2$ and the number of neutron boson holes by $N_\nu=(82-N_n)/2$.

The range of the adjustable parameters was not exhaustive in this work. Rather, advantage was taken of the work of others[30] whose calculations have limited the values severely. The procedures were as follows.

(1) First, we chose to set $\chi_\pi$, $c_\nu^{(0)}$, and $c_\pi^{(0)}=0$. We chose to set $c_\nu^{(1)}=c_\pi^{(1)}=0.1$ MeV. Thus the number of remaining adjustable parameters was reduced from 13 to 8.

(2) We chose $\xi_1=\xi_3=-0.09$ and $\xi_2=0.12$ MeV, as in Ref. 33. These parameters control the position of the mixed-symmetry states (e.g., the $2_3$ level) and have been used previously to push these states to energies of about 2 MeV, above the lower-energy members of the ground and gamma bands.[32] Our investigation showed that indeed the $2_3$ level was pushed to about 1.9 MeV. The set used by Puddu *et al.*, $\xi_1=\xi_2=0.12$ and $\xi_3=-0.09$ (not their $-0.9$), gives the same results. However, the set of Otsuka and Ginocchio,[34] $\xi_1=\xi_3=0.1-0.6$ and $\xi_2=0.0$, used for $^{148,154}$Sm was not satisfactory for our region, which required a $\xi_2$ which is positive. Thus the number of remaining adjustable parameters was reduced to five parameters.

(3) For each nucleus, initial values of $\epsilon_d$, $\kappa$, $\chi_\nu$, and $c_\nu^{(2)}=c_\pi^{(2)}$ were taken from the curves of Ref. 30. The program NPBOS diagonalized the Hamiltonian and calculated the eigenstate energies. These were compared with the experimental level energies. During repeated calculations, minor changes in the parameters were made in order to obtain acceptable fits to the experimental energy levels. Typically, the $2_g$, $2_\gamma$, and $4_g$ energy levels were fitted to within ±20 keV.

(4) The effective charges of the neutron and proton bosons must be entered into the computation of the $B(E2)$ transition probabilities. The $e_\nu^{(2)}$ and $e_\pi^{(2)}$ were set equal to each other and to 0.12 $e$ b, as in Ref. 30. Then, with no additional adjustments of parameters, these effective charges were used in the computation of the $E2$ transition probabilities. We did not attempt to fit with different proton and neutron effective charges[35,36] because of the limited quantity of data for these nuclei. Note that the ratios which are listed in Table VI are not affected by the choice of effective charge because we have taken the proton and neutron effective charges to be equal.

(5) The $c_\nu^{(2)}=c_\pi^{(2)}$ were adjusted for each nucleus until the ratio $R$ [Eq. (2)] agreed with the experimental value. These parameters were typically $-0.30$ MeV, with individual values from $-0.25$ to $-0.40$ MeV. Small changes in the other parameters were made to correct for energy shifts. The effect of $c_\pi^{(2)}$ was significant for $N_n=76$ and 78, but had much less effect for the lighter nuclei with greater number of neutron-hole bosons.

(6) The final values of $\epsilon_d$ varied almost linearly from 0.42 to 0.90 MeV as $N_n$ was varied from 68 to 78 for the Ce nuclei; the Nd and Sm nuclei followed the same curve except for minor differences. $\kappa$ was usually $-0.200$ MeV, with individual variations from $-0.174$ to $-0.420$ MeV. $\chi_\nu$ varied linearly from 0.25 to 0.40 for $N_n=68-74$ for Ce; the Nd and Sm nuclei followed the same curve except for minor differences.

Table VI displays the results as ratios of the calculated $B(E2)$'s compared to the experimental ratios. The same data are not available for each of the nuclei in Table VI. In addition to those nuclei for which the $B(E2;0_g^+ \rightarrow 2_g^+)$ is known and the ground-state band and some of the gamma-band energies are known, there are (a) nuclei for which the $B(E2)$ and the ground-state band energies are known, but there are no known gamma-band level ener-

TABLE VI. Results of the IBM-2 calculations of $B(E2)$ ratios, given in percent and compared with experimental results. $g$ and $\gamma$ indicate the ground-state band and the gamma band, respectively. Uncertainties are given in parentheses. Data without references are from this work.

| | $\frac{B(E2;2_\gamma \rightarrow 0_g)}{B(E2;2_\gamma \rightarrow 2_g)}$ | | $\frac{B(E2;3_\gamma \rightarrow 2g)}{B(E2;3_\gamma \rightarrow 2_\gamma)}$ | | $\frac{B(E2;3_\gamma \rightarrow 4_g)}{B(E2;3_\gamma \rightarrow 2_\gamma)}$ | | $\frac{B(E2;4_\gamma \rightarrow 2_g)}{B(E2;4_\gamma \rightarrow 2_\gamma)}$ | |
|---|---|---|---|---|---|---|---|---|
| Nucleus | Theory | Expt. (%) | Theory | Expt. (%) | Theory | Expt. (%) | Theory | Expt. (%) |
| $^{126}$Ce[a] | 15.8 | | 9.55 | | 20.3 | | 0.77 | |
| $^{128}$Ce[a] | 13.2 | | 9.11 | | 21.9 | | 0.69 | |
| $^{130}$Ce | 9.86 | 12.6 (1.9) | 8.23 | 9.7 (3.1) | 24.5 | 27.6 (12.0) | 0.53 | |
| $^{132}$Ce | 4.65 | 6.0 (1) | 5.36 | 5.6 (0.9) | 29.9 | | 0.31 | |
| $^{134}$Ce | 2.57 | 7.8 (2.5)[b] | 3.19 | 3.6 (1.0)[b] | 32.1 | | 0.27 | |
| $^{136}$Ce[c] | 0.92 | 1.0 (0.1)[d] | 1.11 | 1.5 (0.2)[d] | 33.9 | | 0.28 | |
| $^{132}$Nd | 12.3 | 20.5 (4.4) | 8.64 | 2.5 (1.6) | 22.4 | | 0.55 | |
| $^{134}$Nd | 8.66 | 8.4 (0.6) | 7.05 | 5.1 (0.8) | 24.3 | 42.8 (5.8) | 0.59 | |
| $^{136}$Nd | 4.78 | 6.0 (0.5)[e] | 4.66 | 5.3 (0.4)[e] | 28.5 | 48.9 (10.5)[e] | 0.37 | |
| $^{138}$Nd[c] | 1.75 | 1.2 (0.3)[f] | 1.99 | 1.1 (0.2)[f] | 32.7 | | 0.28 | |
| $^{134}$Sm[a] | 19.7 | | 9.13 | | 16.1 | | 1.34 | |
| $^{136}$Sm | 10.7 | 9.3 (2.4)[g] | 7.47 | | 22.5 | 75.1 (35.4)[g] | 0.53 | |
| $^{138}$Sm | 2.98 | 2.1 (0.3)[h] | 3.15 | 2.7 (0.4)[h] | 29.3 | | 0.86 | |
| $^{140}$Sm[c] | 1.68 | | 1.82 | | 31.6 | | 0.81 | |

| | $\frac{B(E2;4_\gamma \rightarrow 4_g)}{B(E2;4_\gamma \rightarrow 2_\gamma)}$ | | $\frac{B(E2;5_\gamma \rightarrow 4_\gamma)}{B(E2;5_\gamma \rightarrow 3_\gamma)}$ | | $\frac{B(E2;5_\gamma \rightarrow 4_g)}{B(E2;5_\gamma \rightarrow 3_\gamma)}$ | | $B(E2;0_g \rightarrow 2_g)$ | |
|---|---|---|---|---|---|---|---|---|
| Nucleus | Theory | Expt. (%) | Theory | Expt. (%) | Theory | Expt. (%) | Theory[l] | Expt. ($e^2b^2$) |
| $^{126}$Ce | 42.3 | | 49.2 | | 5.40 | | 2.52 | 2.46 (0.13)[j] |
| $^{128}$Ce | 44.6 | | 47.8 | | 5.01 | | 2.15 | 2.15 (0.18)[k] |
| $^{130}$Ce | 49.3 | 46.6 (13.4) | 46.6 | | 4.37 | | 1.80 | 1.73 (0.09)[k] |
| $^{132}$Ce | 61.9 | 104.0 (38.8) | 45.9 | | 2.66 | | 1.46 | 1.77 (0.14)[k,l] |
| $^{134}$Ce | 69.2 | 45.7 (14.1)[b,m] | 45.9 | | 1.33 | | 1.13 | 1.03 (0.09)[k] |
| $^{136}$Ce | 73.6 | | 45.1 | | 0.41 | | 0.77 | 0.8[c] |
| $^{132}$Nd | 40.4 | | 50.2 | | 5.60 | | 2.16 | 2.50 (0.20)[n] |
| $^{134}$Nd | 50.4 | 42.8 (5.8) | 47.6 | | 3.59 | | 1.75 | 1.56 (0.12)[o] |
| $^{136}$Nd | 53.3 | 85.2 (26.5)[e] | 48.3 | 51.3 (14.8)[e] | 2.59 | 4.1 (0.5)[e] | 1.41 | $>0.50$[p] |
| $^{138}$Nd | 71.2 | 66.8 (8.7)[f] | 45.1 | | 0.76 | | 1.03 | 0.6[b] |
| $^{134}$Sm | 38.4 | | 56.8 | | 5.88 | | 2.49 | 4.01 (0.32)[q] |
| $^{136}$Sm | 47.7 | | 51.1 | | 3.79 | | 2.09 | 2.16 (0.15)[r] |
| $^{138}$Sm | 61.3 | 118 (16.7)[h] | 47.0 | | 1.81 | 3.3 (0.5)[h] | 1.51 | 1.64 (0.34)[k] |
| $^{140}$Sm | 68.9 | | 47.9 | | 1.10 | | 1.16 | 1.2[c] |

[a] $B(E2;0_g \rightarrow 2_g)$ is known; no gamma-band levels available.
[b] Data from Ref. 41.
[c] $B(E2;0_g \rightarrow 2_g)$ not known; used extrapolated value.
[d] Data from Ref. 42.
[e] Data from Ref. 18.
[f] Data from Ref. 39.
[g] Data from Ref. 14.
[h] Data from Refs. 43, 44.
[l] With neutron and proton effective charges $=0.129e$ b.
[j] From Ref. 45.
[k] From Ref. 37.
[l] From Ref. 49.
[m] Using one-half of a doublet intensity.
[n] Weighted average from Refs. 8, 45, and 46.
[o] Average from Refs. 46 and 47.
[p] From Ref. 47.
[q] From Ref. 46.
[r] Average from Refs. 8, 46, and 48.

TABLE VII. Davydov and Filippov (Ref. 40) predicted that for the level energies in a rigid triaxial nucleus, $E(2_g^+)+E(2_\gamma^+)-E(3_\gamma^+)=0$. For the available data in this region this expression is shown normalized and as a percentage. Note that for equal numbers of neutrons, the values are almost identical, except for $^{136}$Sm, $^{140}$Sm, and $^{140}$Gd.

| Number of neutrons | $[E(2_g)+E(2_\gamma)-E(3_\gamma)]/[E(2_g)+E(2_\gamma)]$ (%) | | | |
|---|---|---|---|---|
| 72 | $^{130}$Ce −8.2 | $^{132}$Nd −7.8 | | |
| 74 | $^{132}$Ce −4.5 | $^{134}$Nd −3.9 | $^{136}$Sm −20.9[a] | |
| 76 | $^{134}$Ce −0.58 | $^{136}$Nd +0.41 | $^{138}$Sm +0.80 | $^{140}$Gd −2.6 |
| 78 | $^{136}$Ce +5.5 | $^{138}$Nd +5.4 | $^{140}$Sm −5.1 | |

[a]The 1034.6-keV level (Ref. 23) as a possible $3_\gamma^+$ level fits with ratio equal to −6.6%.

gies, and (b) nuclei for which there are known ground-state and gamma-band level energies, but no known $B(E2)$. It was assumed that the $\gamma$-ray transitions are purely $E2$ transitions, for the purposes of these comparisons. The magnitudes and the trend with neutron number of the ratios are in good agreement with those in the calculations[30] for Ce. They are also very similar to the experimental results[19] for Ba and Xe.

In the last two columns is a comparison between the calculated and experimental $B(E2;0_g^+\rightarrow 2_g^+)$. The latter are from the compilation of Raman *et al.*,[37] or from other published works as noted, or were derived from published experimental mean lifetimes by use of the Moskowski relationship[38]

$$B(E2;0_g^+\rightarrow 2_g^+)_{\rm up}=5\{56.56[E_\gamma^5 T_{1/2}(E2)]^{-1}\}\ , \quad (3)$$

where the energy is in keV, the half-life in seconds, and the $B(E2)$ in $e^2b^2$ units. The agreement of the calculated $B(E2;0_g^+\rightarrow 2_g^+)$ values with the available experimental ones were surprisingly satisfactory. They were calculated with effective charges equal to $0.12e$ b. These $B(E2)$ were generally smaller than the experimental $B(E2)$; a larger effective charge was required. Because the same effective charge was used for protons and neutrons, and because the $B(E2)$ are proportional to the square of the effective charges, a best fit of the calculated values to the experimental values could be made simply. A minimum chi-squared adjustment factor of 1.156 was determined and applied to each calculated $B(E2;0_g\rightarrow 2_g)$. The adjusted effective charges were $0.129e$ b. The adjusted $B(E2)$ are listed in Table VI.

It is interesting to observe that the $B(E2)$ ratios can assist in the determination of the spin of a gamma-band level (subject to the applicability of the model). For example, in the $^{138}$Nd data[39] there are two candidates for the $4_\gamma^+$ level, at 1800.0 and 1842.9 keV. The 1842.9-keV level has transitions to the $4_g^+$ and the $2_\gamma^+$ levels; the experimental relative $B(E2)$ of 66.7% is in good agreement with the computed 71.2% of Table VI. By contrast, the 1800.0-keV level has transitions to the $2_g^+$ and the $2_\gamma^+$ levels with an experimental relative $B(E2)$ of 107%, which is approximately 300 times larger than the computed value 0.28; hence this assignment can be rejected.

### B. Comparison with the rigid rotator

A comparison is now made with the criterion of Davydov and Filippov[40] for an asymmetric rotator which

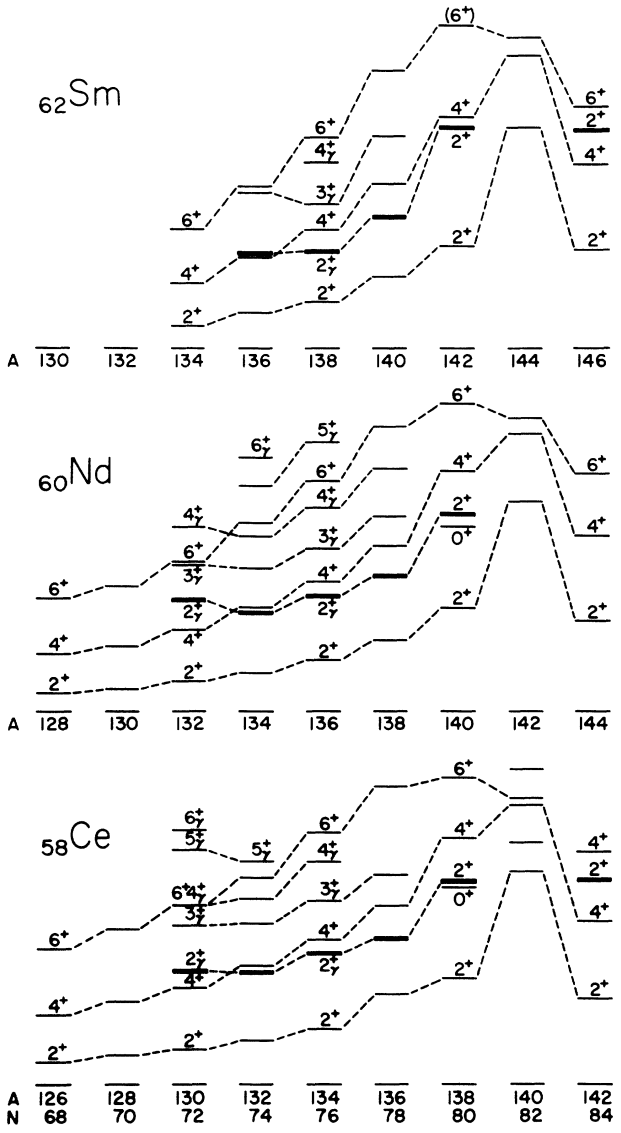


FIG. 9. Systematic comparison of low-lying energy levels of Ce, Nd, and Sm in the region with $68\leq N\leq 84$. Note that as the ground-state band members decrease in energy with the decrease in neutron number (i.e., with increase in the number of neutron holes), the gamma-band members cease following the decreasing energy pattern at $N=72-74$, indicating a change toward a less-soft structure.

rotates without changes in its internal structure, namely, that level energies are expected to obey $E(2_g^+)+E(2_\gamma^+)=E(3_\gamma^+)$. Normalized ratios (expected to be zero) which embody this equation,

$$[E(2_g^+)+E(2_\gamma^+)-E(3_\gamma^+)]/[E(2_g^+)+E(2_\gamma^+)] , \quad (4)$$

are given in Table VII for the nuclei of this study and other adjacent ones. We see that the ratios are equal to zero within $\pm 10\%$. Inequality is expected for gamma-soft nuclei. The similarity of the ratios for each $N$ indicates the strong dependence of the shape on neutron number. The small ratios for the $N=76$ nuclei suggest that they are more rigid that their neighbors. Such a prediction of approximate triaxial rigidity was made by Leander and Nazarewiez in Ref. 23, for the $N=76$ group, $^{134}$Ce, $^{136}$Nd, $^{138}$Sm, and $^{140}$Gd, with $\gamma=17°$, 20°, 23°, and 20°, respectively, and with significant potential barriers relative to $\gamma=0°$ and 60°. However, adjacent $^{140}$Sm, with $\gamma=25°$ and higher potential barriers, was predicted to be the best candidate for being a rigid triaxial nucleus. The radical departure from zero of the criterion of Eq. (4) for $^{136}$Sm (i.e., $-20.6\%$) appears as a contradiction to the systematic trends of the other nuclei.

## V. SUMMARY

It has been evident for several years that the ground-state rotational bands for nuclei with $Z$ near 58 and $N_n < 82$ indicate increasing deformation with decreasing neutron number, with only a weak dependence on the proton number. Available data which illustrate this behavior for the Ce, Nd, and Sm nuclei are shown in Fig. 9. The $2_\gamma^+$ band heads have been accented to emphasize the gamma bands, which include our data and other available data. These nuclei become less "soft" and the levels of the gamma bands go up in energy relative to the ground-state bands, as the neutron number decreases.

The systematic trends of the energy levels and the $B(E2)$ ratios, dependent on neutron number, are very similar to those which were observed in Xe and Ba nuclei,[19] and indicate that there are no radical changes in structure with the change in proton number from 54 to 62. Overall, the reasonable agreement of the IBM-2 calculated values with the experimental ones supports the applicability of IBM-2 to these transitional nuclei.

## ACKNOWLEDGMENTS

The authors gratefully acknowledge the assistance of H. K. Carter and C. P. Perez. G. A. Leander kindly discussed many questions with the authors. UNISOR is a consortium of universities, state of Tennessee, Oak Ridge Associated Universities, and Oak Ridge National Laboratory, and is partially supported by them and the U.S. Department of Energy under Contract No. DE-AC05-OR00033 with Oak Ridge Associated Universities. Other support was provided by the Department of Energy under Contract Nos. DE-AS05-76ER03346 (Georgia Institute of Technology) DE-AC05-84OR21400 (Oak Ridge National Laboratory) and DE-FG05-84ER40159 (Louisiana State University) and by the Southern Regional Education Board (University of Kentucky).

*Present address: Department of Physics, University of Jyvaskyla, 40100 Jyvaskyla, Finland.

†Present address: Physics Department, Jadwin Hall, Princeton University, Princeton, NJ 08544.

‡Present address: Environmental Compliance and Health Protection Division, Oak Ridge National Laboratory, Oak Ridge, TN 37831.

[1]R. K. Sheline, T. Sikkeland, and R. N. Chanda, Phys. Rev. Lett. 7, 446 (1961).

[2]I. Ragnarsson, A. Sobiczewski, R. K. Sheline, S. E. Larsson, and B. Nerlo-Pomorska, Nucl. Phys. **A233**, 329 (1974).

[3]G. A. Leander and P. Möller, Phys. Lett. **110B**, 17 (1982).

[4]I. Ragnarsson and R. K. Sheline, Phys. Scr. **29**, 385 (1984).

[5]R. Bengtsson, P. Möller, J. R. Nix, and Jing-ye Zhang, Phys. Scr. **29**, 402 (1984).

[6]David Ward, R. M. Diamond, and F. S. Stephens, Nucl. Phys. **A117**, 309 (1968).

[7]W. Dehnhardt, S. J. Mills, M. Müller-Veggian, U. Neumann, D. Pelte, G. Poggi, B. Povh, and P. Taras, Nucl. Phys. **A225**, 1 (1974).

[8]A. Makishima, M. Adachi, H. Taketani, and M. Ishii, Phys. Rev. C **34**, 576 (1986).

[9]C. J. Lister, B. J. Varley, R. Moscrop, W. Gelletly, P. J. Nolan, D. J. G. Love, P. J. Bishop, A. Kirwan, D. J. Thornley, L. Ying, R. Wadsworth, J. W. O'Donnell, H. G. Price, and A. H. Nelson, Phys. Rev. Lett. **55**, 810 (1985).

[10]H. R. Hiddleston and C. P. Browne, Nucl. Data Sheets **13**, 133 (1974); **17**, 225 (1976).

[11]Yu. V. Sergeenkov and V. M. Sigalov, Nucl. Data Sheets **34**, 475 (1981).

[12]*Table of Isotopes*, edited by C. D. Lederer and V. S. Shirley (Wiley, New York, 1978).

[13]R. Béraud, A. Charvet, R. Duffait, A. Emsallem, J. Genevey, A. Gizon, M. Meyer, N. Redon, and D. Rolando-Eugio, in *Nuclei Far from Stability*, Proceedings of the 5th International Conference on Nuclei Far from Stability, Rosseau Lake, Ontario, Canada, 14–19 September, 1987, edited by I. S. Towner (AIP, New York, 1988), pp. 445ff.

[14]K. S. Vierinen, J. M. Nitschke, P. A. Wilmarth, R. B. Firestone, and J. Gilat, Nucl. Phys. **A499**, 1 (1989).

[15]R. Wadsworth, J. M. O'Donnell, D. J. Watson, P. J. Nolan, A. Kirwan, P. J. Bishop, M. J. Godfrey, D. J. Thornley, and D. J. G. Love, J. Phys. G **14**, 239 (1988).

[16]P. J. Nolan, R. Aryaeinejad, D. J. G. Love, A. H. Nelson, P. J. Smith, D. M. Todd, P. J. Twin, J. D. Garrett, G. B. Hagemann, and B. Herskind, Phys. Scr. T **5**, 153 (1983).

[17]M. Kortelahti, E. F. Zganjar, R. L. Mlekodaj, B. D. Kern, R. A. Braga, R. W. Fink, and C. P. Perez, Z. Phys. A **327**, 231 (1987).

[18]B. D. Kern, R. L. Mlekodaj, M. O. Kortelahti, R. A. Braga, and R. W. Fink, Z. Phys. A **330**, 37 (1988).

[19]R. F. Casten and P. von Brentano, Phys. Lett. **152**, 22 (1985).

[20]H. K. Carter, E. H. Spejewski, R. L. Mlekodaj, A. G. Schmidt, F. T. Avignone, C. R. Bingham, R. A. Braga, J. D. Cole, A. V. Ramayya, J. H. Hamilton, E. L. Robinson, K. S. R. Sastry, and E. F. Zganjar, Nucl. Instrum. Methods **139**, 349 (1976).

[21]E. H. Spejewski, R. L. Mlekodaj, and H. K. Carter, Nucl. Instrum. Methods **186**, 71 (1981).

[22]R. L. Mlekodaj, E. F. Zganjar, and J. D. Cole, Nucl. Instrum. Methods **186**, 239 (1981).

[23]B. D. Kern, R. L. Mlekodaj, G. A. Leander, M. O. Kortelahti, E. F. Zganjar, R. A. Braga, R. W. Fink, C. P. Perez, W. Nazarewicz, and P. B. Semmes, Phys. Rev. C **36**, 1514 (1987).

[24]R. Wadsworth, S. M. Mullins, J. R. Hughes, P. J. Nolan, A. Kirwan, P. J. Bishop, I. Jenkins, M. J. Godfrey, and D. J. Thornley, J. Phys. G **15**, L47 (1989).

[25]D. D. Bogdanov, A. V. Demyanov, V. A. Karnaukhov, L. A. Petrov, A. Plohocki, V. G. Subbotin, and J. Voboril, Nucl. Phys. **A275**, 229 (1977).

[26]A. H. Wapstra and K. Bos, At. Data Nucl. Data Tables **19**, 177 (1977).

[27]P. A. Wilmarth, J. M. Nitschke, P. K. Lemmertz, and R. B. Firestone, Z. Phys. A **321**, 179 (1985).

[28]D. Barnéoud, J. Blachot, J. Genevey, A. Gizon, R. Béraud, R. Duffait, A. Emsallem, M. Meyer, N. Redon, and D. Rolando-Eugio, Z. Phys. A **330**, 341 (1988).

[29]D. M. Todd, R. Aryaeinejad, D. J. G. Love, A. H. Nelson, P. J. Nolan, P. J. Smith, and P. J. Twin, J. Phys. G **10**, 1407 (1984).

[30]G. Puddu, O. Scholten, and T. Otsuka, Nucl. Phys. **A348**, 109 (1980).

[31]T. Otsuka and N. Yoshida, Japan Atomic Energy Research Institute, Tokai, Ibaraki, Japan, Report No. JAERI-M-85-094, 1985.

[32]A. Arima and F. Iachello, in *Advances in Nuclear Physics*, edited by J. W. Negele and Eric Vogt (Plenum, New York, 1984), Vol. 13, p. 139.

[33]M. Sambataro, Nucl. Phys. **A380**, 365 (1982).

[34]Takaharu Otsuka and Joseph N. Ginocchio, Phys. Rev. Lett. **54**, 777 (1985).

[35]W. D. Hamilton, A. Irbäck, and J. P. Elliott, Phys. Rev. Lett. **53**, 2469 (1984).

[36]O. Scholten, R. M. Ronningen, A. Y. Ahmed, G. O. Bomar, H. L. Crowell, J. H. Hamilton, H. Kawakami, C. F. Maguire, W. G. Nettles, R. B. Piercey, A. V. Ramaya, R. Soundranayagam, and P. H. Stelson, Phys. Rev. C **34**, 1962 (1986).

[37]S. Raman, C. H. Malarkey, W. T. Milner, C. W. Nestor, Jr., and P. H. Stelson, At. Data Nucl. Data Tables **36**, 1 (1987).

[38]K. E. G. Löbner, M. Vetter, and V. Hönig, Nucl. Data Tables A **7**, 495 (1970).

[39]J. Deslauriers, S. C. Gujrathi, and S. K. Mark, Z. Phys. A **303**, 151 (1981).

[40]A. S. Davydov and G. F. Filippov, Nucl. Phys. **8**, 237 (1958).

[41]M. Müller-Veggian, H. Béuscher, D. R. Haenni, R. M. Lieder, and A. Neskakis, Nucl. Phys. **A417**, 189 (1984).

[42]T. W. Burrows, Nucl. Data Sheets **52**, 273 (1987).

[43]A. Charvet, T. Ollivier, R. Béraud, R. Duffait, A. Emsallem, N. Idrissi, J. Genevey, and A. Gizon, Z. Phys. A **321**, 697 (1985).

[44]N. Redon, T. Ollivier, R. Béraud, A. Charvet, R. Duffait, A. Emsallem, J. Honkanen, M. Meyer, J. Genevey, A. Gizon, and N. Idrissi, Z. Phys. A **325**, 127 (1986).

[45]R. Moscrop, M. Campbell, W. Gelletly, L. Goettig, C. J. Lister, B. J. Varley, and H. G. Price, Nucl. Phys. **A481**, 559 (1988); *Proceedings of the International Physics Conference*, Harrogate, U.K., 1986 (IOP, Bristol, 1986), Vol. 1, p. 160.

[46]R. Wadsworth, J. M. O'Donnell, D. L. Watson, P. J. Nolan, P. J. Bishop, D. J. Thornley, A. Kirwan, and D. J. G. Love, J. Phys. G **13**, 205 (1987).

[47]J. Billowes, K. P. Lieb, J. W. Noè, W. F. Piel, Jr., S. L. Rolston, G. D. Sprouse, O. C. Kistner, and F. Christancho, Phys. Rev. C **36**, 974 (1987).

[48]F. Soramel, S. Lunardi, S. Beghini, M. Morando, G. Signorini, W. Meczynski, G. Fortuna, G. Montagnoli, and A. M. Stefanini, Phys. Rev. C **38**, 537 (1988).

[49]A. J. Kirwan, P. J. Bishop, D. J. G. Love, P. J. Nolan, D. J. Thornley, A. Dewald, A. Gelberg, K. Schiffer, and K. O. Zell, J. Phys. G **15**, 85 (1989).